## Orbital Optimization and Neural-Network-Assisted Configuration Interaction Calculations of Rydberg States

Gianluca Levi,\*,†,‡ Max Kroesbergen,¶ Louis Thirion,¶,† Yorick L. A. Schmerwitz,†,§ Elvar Ö. Jónsson,† Pavlo Bilous,∥ Philipp Hansmann,\*,¶,† and Hannes Jónsson\*,†

 $\dagger Science\ Institute\ and\ Faculty\ of\ Physical\ Sciences,\ University\ of\ Iceland,\ Reykjavík,\\ Iceland$ 

‡Department of Chemical and Pharmaceutical Sciences, University of Trieste, 34127 Trieste, Italy

¶Department of Physics, Friedrich-Alexander-Universität Erlangen/Nürnberg, 91058 Erlangen, Germany

§Max-Planck-Institut für Kohlenforschung, 45470 Mülheim an der Ruhr, Germany ||Max Planck Institute for the Science of Light, Staudtstraße 2, 91058 Erlangen, Germany

E-mail: gianluca.levi@units.it; philipp.hansmann@fau.de; hj@hi.is

#### Abstract

Rydberg excited states of molecules pose a challenge for electronic structure calculations because of their highly diffuse electron distribution. Even large and elaborate atomic basis sets tend to underrepresent the long-range tail, overly confining the Rydberg state. An approach is presented where the molecular orbitals are variationally optimized for the excited state using a plane wave basis set in Hartree-Fock calculations, followed by configuration interaction calculations on the resulting reference. Using excited state optimized plane wave orbitals greatly enhances the convergence of the many-body calculation, as illustrated by a full configuration interaction calculation of the 2sRydberg state of H<sub>2</sub>. A neural-network-based selective configuration interaction approach is then applied to calculations of the 3s,  $3p_x$  and  $3p_y$  states of H<sub>2</sub>O and the 3s and  $3p_z$  states of NH<sub>3</sub>. The obtained values of excitation energy are in close agreement with experimental measurements as well as previous many-body

calculations based on sufficiently diffuse atomic basis sets. Previously reported high-level calculations limited to atomic basis sets lacking extra diffuse functions, such as aug-cc-pVTZ, give significantly higher estimates due to confinement of the Rydberg states.

#### 1 Introduction

The accurate description of Rydberg excited states of molecules is a challenge in quantum chemistry because of the highly diffuse electron distribution. The energy of a set of Rydberg states of a molecule follows roughly the Rydberg series analogous to that of the hydrogen atom because the excited electron is subject to an effective potential consistent with an unscreened charge of nearly +e. For several molecules, such as NH<sub>3</sub> and H<sub>2</sub>O, even the first excited state is a Rydberg state. While time-dependent density functional theory (TDDFT) and equation-of-motion coupled cluster (EOM-CC) methods are widely used in calculations of

excited states, they often struggle with calculations of Rydberg excited states due to limitations in the atomic orbital basis and approximations in the treatment of electron correlation. <sup>1,2</sup> Accurate calculations of Rydberg states require special basis sets where extra diffuse functions have been added, as well as multi-reference representation of the wave function. <sup>3–5</sup>

The application of Kohn-Sham DFT to Rydberg states is problematic because of the incorrect long-range form of the effective potential resulting from the self-interaction in the estimation of the classical electron-electron interaction from the total electron density. Recently, however, it has been demonstrated that orbitaloptimized calculations using density functionals with explicit self-interaction corrections (SIC) can give remarkably accurate description of molecular Rydberg states. 6 There, the convergence on excited states is obtained by converging to a saddle point on the electronic energy surface.<sup>7–9</sup> Furthermore, by using a real-space grid or plane wave representation, the diffuse nature of the Rydberg orbital can be represented better than with conventional diffuse atomic basis sets. While such calculations provide an improved mean-field description, a more rigorous many-body treatment is required to accurately capture electron correlation effects in excited states and provide benchmarks for calibrating less accurate and faster methods.

In a recent study, we presented a neuralnetwork (NN)-based selective configuration interaction (CI) approach to calculations of many-body wave functions for molecules. <sup>10</sup> The NNCI approach is based on an iterative classification of Slater determinants as relevant or irrelevant for the convergence of a chosen observable. In calculations of the ground state energy of molecules, it was found that NNCI is able to capture the full correlation energy obtained by full CI results with several orders of magnitude fewer determinants. One of the key insights from this work is that an increase in the number of molecular orbitals (MOs) beyond what can be included in a typical full CI calculation improved significantly the accuracy of the results.

Building on these findings, here the NNCI

approach is extended to calculations of excited electronic states, and applied to Rydberg states of molecules. A state-specific strategy is adopted, where the MOs are variationally optimized in plane wave-based Hartree-Fock calculations, and the resulting orbitals used in an NNCI calculation of the target excited state. The use of state-specific optimized orbitals has previously been shown to improve the results of CI calculations of excited states that account for single and double excitations (CISD) and using basis sets of localized atomic orbitals. 11,12 Here, a plane wave orbital representation is used in the Hartree-Fock calculations, ensuring full flexibility and an adequate description of the highly diffuse Rydberg states. Moreover, the CI calculations are not limited to single and double excitations, but the full Hilbert space is explored within the selective NNCI approach.

The advantage of using plane wave based Hartree-Fock orbitals optimized for the excited state is first illustrated in full CI calculations of the 2s Rydberg state of the H<sub>2</sub> molecule. Then, the excited state NNCI approach is applied to Rydberg excitations of the NH<sub>3</sub> and H<sub>2</sub>O molecules, especially those that have previously turned out to be challenging for typical quantum chemistry calculations.<sup>3-6</sup>

#### 2 Methods

The Rydberg excited-state calculations are performed by first converging either the ground or a target excited state in a Hartree–Fock calculation using a plane wave basis to represent the occupied orbitals. The resulting Hartree–Fock MOs are then used as the basis for a subsequent CI calculation. For the H<sub>2</sub> molecule, a full CI calculation is performed, while for the NH<sub>3</sub> and H<sub>2</sub>O molecules, the NNCI method is applied in a state-specific manner targeting the desired excited state. All calculations are performed by retaining spin symmetry.

#### 2.1 Hartree-Fock Excited States

The Hartree-Fock calculations use the projector augmented wave (PAW) method  $^{13,14}$  to treat

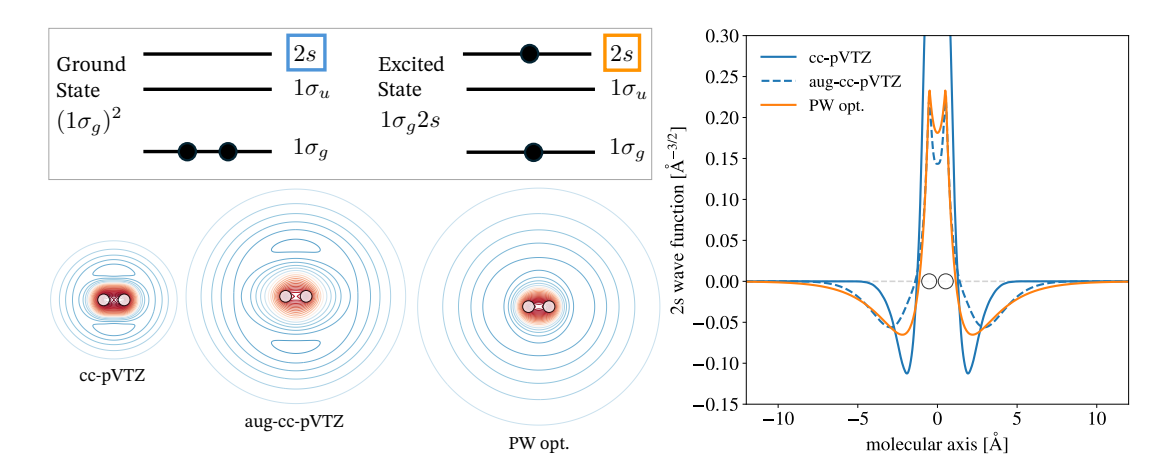


Figure 1: Top left: Orbital occupation in the spin restricted Hartree-Fock calculation of the ground and 2s Rydberg excited states of the  $H_2$  molecule. Bottom left and right: Comparison of the 2s Rydberg orbital obtained in three different calculations, displayed as contour maps (red and blue lines corresponding to regions of positive and negative amplitude, respectively) and amplitude along the molecular axis. In a ground state Hartree-Fock calculation initialized using the cc-pVTZ (blue solid line) or aug-cc-pVTZ (blue dashed line) basis set, the 2s orbital has shorter tails than in an excited state calculation where the occupied orbitals are variationally optimized for the 2s Rydberg state (orange curve). In each case, the occupied orbitals are represented by a plane wave basis, but the unoccupied orbitals are largely determined by the atomic basis set used in the initialization. Circles mark the positions of the protons.

the electrons near the nuclei, with core electrons frozen to the states obtained in scalar relativistic calculations of the isolated atoms. The MOs for the valence electrons are initialized using a localized atomic orbital basis of primitive Gaussian functions from the cc-pVTZ or aug-cc-pVTZ sets, <sup>15,16</sup> with an additional set of numerical s-type atomic orbitals. <sup>17,18</sup> Occupied orbitals are then variationally optimized in a plane wave representation, while unoccupied orbitals are only modified through the orthogonalization to the optimized occupied orbitals.

The Hartree-Fock ground singlet state is obtained by minimizing the energy in a spin-restricted calculation using an L-BFGS algorithm, <sup>19</sup> thereby converging on a solution with aufbau orbital occupation. For the excited state Hartree-Fock calculations, the orbitals are initialized using the ground state orbitals setting the occupations numbers of the HOMO and the target excited orbital to 1. This corresponds to promotion of an electron from the HOMO to the target excited orbital within the spin-restricted representation. While this orbital occupation does not correspond to a pure excited

state, it ensures that the Rydberg orbital is variationally optimized in the plane wave basis set. The occupied orbitals are optimized, converging either to a local minimum (for the HOMO-LUMO excitation) or to a saddle point. The saddle point optimization is performed using a direct optimization method<sup>8</sup> employing a limited-memory version of the symmetric rankone (L-SR1) quasi-Newton algorithm.<sup>9</sup>

The Hartree-Fock calculations make use of a grid spacing of 0.18 Å and a plane wave energy cutoff of 1000 eV. The simulation cell includes at least 10 Å of vacuum between each atom and the nearest cell boundary. The calculations are performed with a development version of the GPAW software.<sup>20</sup> The atomic coordinates of the molecules are taken from ref. 21.

#### 2.2 NN-assisted CI

For the calculation of the many-body wave functions, the Hamiltonian is cast into the form

$$H = H^{0} + H^{\text{int}} - MF \left[H^{\text{int}}\right]$$
 (1)

where

$$H^{0} = \sum_{i,j,\sigma} t_{ij} c_{i,\sigma}^{\dagger} c_{j,\sigma} \tag{2}$$

$$H^{\text{int}} = \sum_{\substack{i,j,k,l \\ \sigma'}}^{i,j,b} U_{ijkl} \ c_{i,\sigma}^{\dagger} c_{j,\sigma} c_{k,\sigma'}^{\dagger} c_{l,\sigma'}. \tag{3}$$

(4)

Here,  $c_{i,\sigma}^{\dagger}$  and  $c_{i,\sigma}$  are fermionic (creation/annihilation) field operators with orbital and spin indices i and  $\sigma$ , respectively. The  $t_{ij}$  and  $U_{ijkl}$  are the single- and two-particle integrals

$$t_{ij} \equiv \int d\mathbf{r} \varphi_i^*(\mathbf{r}) \left( -\frac{1}{2} \nabla^2 + V^{\text{eff}}(\mathbf{r}) \right) \varphi_j(\mathbf{r})$$

$$(5)$$

$$U_{ijkl} \equiv \int d\mathbf{r} d\mathbf{r}' \varphi_i^*(\mathbf{r}) \varphi_j(\mathbf{r}) \frac{1}{|\mathbf{r} - \mathbf{r}'|} \varphi_k^*(\mathbf{r}') \varphi_l(\mathbf{r}')$$

$$(6)$$

where  $V_{\text{eff}}(\mathbf{r})$  is the self-consistent mean-field potential, and the integrals are evaluated using the excited state optimized Hartree-Fock orbitals  $\varphi_i(\mathbf{r})$ . The term MF  $[H^{\text{int}}]$  in Eq. (1), is the mean-field decoupled interaction operator. Since its contributions are implicitly included in the Hartree-Fock single particle integrals,  $t_{ij}$ , it needs to be subtracted in order to avoid double counting.

All the CI and NNCI computations were performed using the SOLAX package, <sup>22</sup> a Python library designed to compute and analyze fermionic quantum systems using the formalism of second quantization with built-in machine learning support, with orbitals and matrix elements obtained in the Hartree-Fock calculations using the GPAW software.

Selective CI - The exact many-body eigenstates,  $|\Psi_{\alpha}\rangle$ , fulfill the eigenvalue equation for Hamiltonian (1)

$$H|\Psi_{\alpha}\rangle = E_{\alpha}|\Psi_{\alpha}\rangle \tag{7}$$

and can be expanded in Slater determinants,  $|\phi\rangle$  which form an orthonormal basis  $\{\phi\}$  of the

full Hilbert space  $\mathcal{H}^{\text{full}} = \text{span}(\{\phi\})$ :

$$|\Psi_{\alpha}\rangle = \sum_{\mathcal{H}^{\text{full}}} c_{\phi}^{\alpha} |\phi\rangle \tag{8}$$

In selective CI, this is approximated by working within a subspace  $\mathcal{H}_s \subset \mathcal{H}_{\text{full}}$  with  $\dim(\mathcal{H}_s) \ll \dim(\mathcal{H}_{\text{full}})$ , such that

$$|\Psi_{\alpha}\rangle \approx |\Psi_{\alpha}^{\text{approx}}\rangle = \sum_{\phi \in \mathcal{H}_s} c_{\phi}^{\alpha} |\phi\rangle$$
 (9)

Our iterative protocol for the selective CI procedure starts from a small initial set of determinants,  $\{\phi_{\text{init}}\}$ . The set is then extended by an extension operator  $\hat{\mathcal{O}}$  that projects out of the current subspace of the total Hilbert space and generates new determinants (provided that the set does not span an eigenspace of the operator). In each iteration, the Hamiltonian eigenproblem is solved within the corresponding subspace, yielding an approximate eigenstate wavefunction and total energy whose accuracy improves over successive iterations due to the variational principle. Due to the combinatorial growth in the number of generated configurations, inclusion of all new determinants quickly becomes impractical. Consequently, a selection protocol has to be introduced. Here, a modified version of the NN-based selection from refs 10 and 23 is used, as detailed below. Our previous NNCI calculations of ground electronic states demonstrate that the NN-based selection significantly outperforms simpler truncation schemes, such as the use of an energy cutoff.

**NNCI Iterations** - The NN-assisted selection scheme used here differs from that in Ref. 10, in that it targets a given excited state,  $|\Psi_{\alpha}\rangle$ . It cannot be tracked by energy alone as its relative position among the eigenstates may change during the iterations. Instead the state is identified and followed based on properties such as its molecular orbital occupations and spin symmetry.

In each iteration, after diagonalizing the Hamiltonian in the current subspace, the eigenstates are compared to a *reference pattern* defined by the expected molecular orbital occupation in the target excited state. In the case of

a Rydberg state, this pattern is given by the mean-field solution and involves one electron occupying the highly diffuse orbital. The singlet formed from these configurations remains dominant throughout the iterative refinement. Once identified, the corresponding CI wavefunction  $|\psi_{\rm ex}\rangle$  serves as the basis for constructing the first determinant pool and identifying the target state in further iterations.

Note that, in practice, we can initialize the procedure from a constrained CI calculation in which the highest-lying orbitals are kept unoccupied, i.e. restricting the number of MOs. This typically simplifies the tracking procedure and yields an overall speedup compared to a full calculation that starts from the mean-field determinants only.

#### Algorithm 1 NNCI Iteration

#### 1: Input:

- Target state  $|\Psi_{\alpha}\rangle$  to be converged
- Determinants  $\{\phi\}$  currently in CI expansion
- Pool of candidate determinants  $\{\phi_{\text{pool}}\} = \mathcal{O}\{\hat{\phi}\} \setminus \{\phi\}$
- Target selection size
- ullet Size of the random sample
- 2: Generate random sample  $\{\phi_{\text{rand}}\}\subset \{\phi_{\text{pool}}\}$
- 3: Identify target state  $\alpha$  on  $\{\phi\} \cup \{\phi_{\text{rand}}\}$
- 4: Adjust the cutoff parameter to split  $\{\phi_{\text{rand}}\}$  into important  $\{\phi_{\text{rand}}^{\text{impt}}\}$  and unimportant  $\{\phi_{\text{rand}}^{\text{unimpt}}\}$  classes
- 5: Train NN classifier on  $\{\phi\} \cup \{\phi_{\text{rand}}\}$
- 6: Predict important determinants  $\{\phi_{NN}^{impt}\} \subset \{\phi_{pool}\}$
- 7: Identify target state  $\alpha$  in  $\{\phi\} \cup \{\phi_{\text{NN}}^{\text{impt}}\} \cup \{\phi_{\text{rand}}^{\text{impt}}\}$
- 8: Eliminate false positives from  $\{\phi_{NN}^{impt}\}$
- 9: Identify target state  $\alpha$  in  $\{\phi\} \cup \{\phi_{\text{NN}}^{\text{impt}}\} \cup \{\phi_{\text{rand}}^{\text{impt}}\}$
- 10: Output:

$$\alpha, \{\phi\} \leftarrow \{\phi\} \cup \{\phi_{\mathrm{NN}}^{\mathrm{impt}}\} \cup \{\phi_{\mathrm{rand}}^{\mathrm{impt}}\}$$

In Algorithm 1, the steps following the initialization phase are summarized. Note that the

NNCI calculations are performed separately for the ground and the excited state for a given set of MOs.

#### 3 Results and Discussion

#### 3.1 Full CI for 2s state of H<sub>2</sub>

The advantage of optimizing the orbitals for the excited state in the Hartree-Fock calculation is first illustrated in calculations of the 2s Rydberg state of the H<sub>2</sub> molecule. Here, the full CI basis is tractable directly and no NN-based selection is needed. Fig. 1 shows the occupation of the orbitals in the ground and 2s Rydberg state as well as the shape of the 2s orbital obtained in three different calculations. In a calculation of the ground state,  $(1\sigma_q)^2$ , where the unoccupied 2s orbital is described within the ccpVTZ basis set, the orbital is confined and lacks the long-range tails. With the extended aug-ccpVTZ basis set, a significantly larger spread of the 2s orbital is obtained. But, in a calculation of the excited state,  $1\sigma_g 2s$ , where the occupied 2s orbital is represented by plane waves, the orbital becomes even more diffuse, reflecting more accurately its Rydberg character.

The energy of the 2s Rydberg state obtained in full CI calculations is shown in Fig. 2 as a function of the internuclear separation and the results are compared to the highly accurate theoretical best estimate (TBE) of Kolos, Wolniewicz and Dressler reported in Refs. 24 and 25.

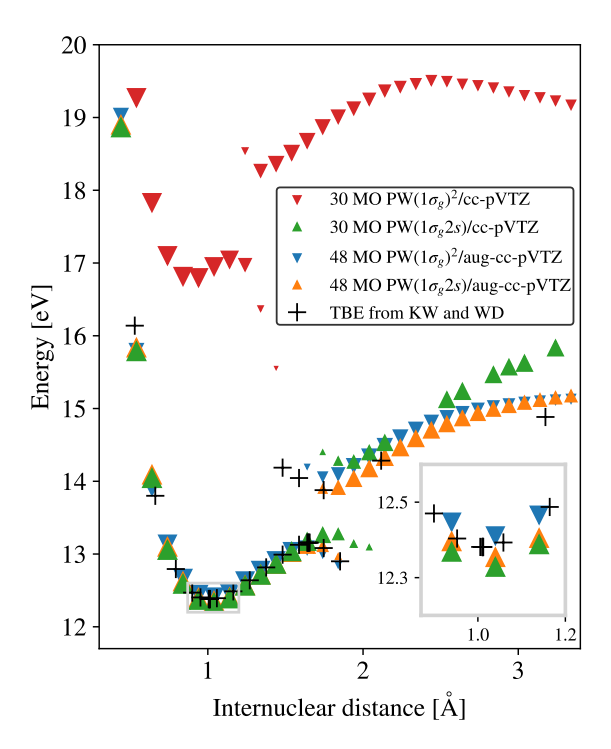


Figure 2: Energy of 2s Rydberg state of  $H_2$  as a function of H-H distance from full CI calculations using different sets of orbitals, with respect to the ground state energy minimum. The occupied orbitals are variationally optimized in Hartree-Fock plane wave (PW) calculations for the ground  $((1\sigma_a)^2$ , downward triangles), or 2sstate  $(1\sigma_q 2s, \text{ upward triangles})$ , while the unoccupied orbitals are represented with the ccpVTZ or aug-cc-pVTZ atomic basis sets used in the initialization. The size of triangles reflects the overlap of the full CI many-body state with the  $1\sigma_q 2s$  two Slater determinant wave function. Inset: Expanded scale around the minimum. Theoretical best estimates (TBE) are from Refs. 24 (KW, lower branch) and 25 (WD, upper branch).

The zero of energy is taken to be the minimum ground state energy. As the H-H bond is stretched, there is an avoided crossing with the  $(1\sigma_u)^2$  state. The size of the triangles is determined by the overlap  $\langle \Psi_{1\sigma_g 2s} | \Psi_{\rm MB} \rangle$ , where  $|\Psi_{\rm MB}\rangle$  are the many-body eigenstates and

$$\left|\Psi_{1\sigma_g 2s}\right\rangle = \frac{1}{\sqrt{2}} \left(\left|1\sigma_g \ \overline{2s}\right\rangle + \left|\overline{1\sigma_g} \ 2s\right\rangle\right) \quad (10)$$

so that the projection indicates the weight of the  $1\sigma_g 2s$  contribution in each of the two branches near the avoided crossing. All states are included in the graph, but states with a negligible overlap are not visible, as a small threshold is imposed.

When the calculations are initialized with the cc-pVTZ basis set with 30 MOs, a large overestimation of the excitation energy is obtained when the occupied orbitals are optimized for the ground state,  $(1\sigma_a)^2$ . At the optimal excited state bond length, the energy with respect to the minimum ground state energy is calculated to be  $\sim 16.7 \,\mathrm{eV}$ , an overestimate by more than 4 eV. This is a result of the strong confinement of the Rydberg orbital as the 2s orbital obtained in the cc-pVTZ basis set lacks the long-range tails. However, when the occupied orbitals are optimized for the 2s Rydberg state,  $1\sigma_q 2s$ , the calculated energy is close to the TBE, with only a slight underestimation of less than 0.1 eV. Furthermore, the position of the avoided crossing with the  $(1\sigma_u)^2$  state is then in good agreement with the TBE, while the calculation with orbitals optimized for the ground state shifts the avoided crossing to a shorter bond distance by about 0.5 Å.

When the aug-cc-pVTZ basis set with 48 MOs is used for the initialization of the Hartree-Fock ground state calculation, the unoccupied 2s Rydberg orbital has significantly longer tails and the calculated energy is improved compared to that obtained with the cc-pVTZ basis set, as can be seen in Fig. 2. The excitation energy, however, remains slightly overestimated, as the tails of the 2s orbital are still not sufficiently extended (see Fig. 1). A further improvement is obtained when the orbitals are optimized for the 2s state instead of the ground state, particularly in the internuclear distance range of 1.5–3 Å. Under this condition, the energy gap at the avoided crossing is reproduced with nearperfect accuracy.

The results shown in Fig. 2 illustrate this. In the ground state calculation, the unoccupied orbitals, and thereby the 2s Rydberg orbital, are not optimized. Instead, they are represented with the cc-pVTZ or aug-cc-pVTZ basis sets and only get adjusted by the orthogonalization to the optimized orbitals. Therefore, the unoccupied 2s Rydberg orbital remains limited by

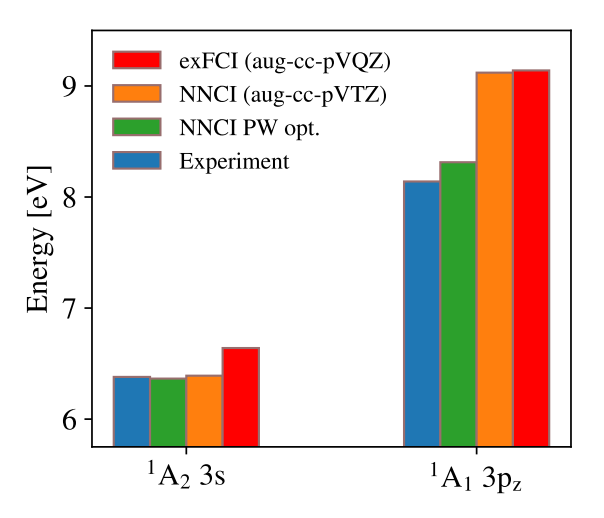


Figure 3: Excitation energy for 3s and  $3p_z$  Rydberg states of the NH<sub>3</sub> molecule calculated with NNCI using 52 MOs, formed initially from the aug-cc-pVTZ basis set, but then optimized variationally for the occupied ones in plane wave based Hartree-Fock calculations, either for the ground state (NNCI aug-cc-pVTZ) or for the target Rydberg state (NNCI PW opt). For comparison, experimental estimates from Refs. 26 and 27 are shown as well as extrapolated full CI calculations (exFCI) from Ref. 4 based on the aug-cc-pVQZ basis set.

the localized nature of the atomic orbitals basis set. In contrast, the plane wave based optimization of the 2s orbital in the excited state Hartree-Fock calculation describes the diffuse nature of the Rydberg state much better and provides significantly improved results.

For larger molecules, a full CI calculation becomes computationally demanding and the NNCI provides an efficient alternative by including only the most important determinants. In excited state calculations, the efficiency is further enhanced by optimizing the Hartree-Fock orbitals for the target state. This is illustrated here in calculations of rather low lying Rydberg states of the NH<sub>3</sub> and H<sub>2</sub>O molecules, and becomes especially clear already for the  $3p_z$  state of NH<sub>3</sub> and the  $3p_x$  state of H<sub>2</sub>O.

### 3.2 NNCI for NH $_3$ Rydberg States

Fig. 3 shows results of NNCI calculations for the 3s and  $3p_z$  Rydberg states of NH<sub>3</sub>. The z-axis is the C<sub>3</sub> rotational symmetry axis. A comparison with experimental measurements from Refs. 26 and 27, as well as reported extrapolated full CI (exFCI) calculations from Ref. 4 is also shown. For both 3s and  $3p_z$  states the NNCI calculated excitation energy is in close agreement with the measured values.

The exFCI calculations are based on the augcc-pVTZ basis and give a slightly higher excitation energy than NNCI for the 3s state and a significantly higher one for the  $3p_z$  state, by about  $0.8\,\mathrm{eV}$ . Even though the NNCI calculation is initialised with the same atomic basis set, the occupied orbitals are variationally optimized for the excited state in the Hartree-Fock calculation, so a better description of the Rydberg state is obtained and fewer determinants are needed in the CI calculation to reach convergence.

The use of ground state orbitals in a CI calculation based on the aug-cc-pVTZ basis set overly confines the Rydberg state and thereby overestimates the excitation energy. This is verified by carrying out the NNCI calculation using the ground state orbitals, which indeed gives a higher estimate of the  $3p_z$  excitation energy, similar to that of the exFCI calculations, as shown in Fig. 3. Again the reason is the missing long-range tail of the  $3p_z$  orbitals obtained from the ground state calculations with the aug-cc-pVTZ basis set.

The limitation of the aug-cc-pVTZ basis set for the  $3p_z$  state of NH<sub>3</sub> has previously been demonstrated in variational density functional calculations where the atomic basis set calculations were compared to calculations carried out with a real space grid, see Figs. 2 and 3 in Ref. 6.

The convergence of the excitation energy with respect to NN iterations is illustrated for both the 3s and  $3p_z$  Rydberg states of NH<sub>3</sub> in Fig. 4. In four cycles of the NN-assisted extension of the set of included determinants and retraining of the NN, convergence is reached already

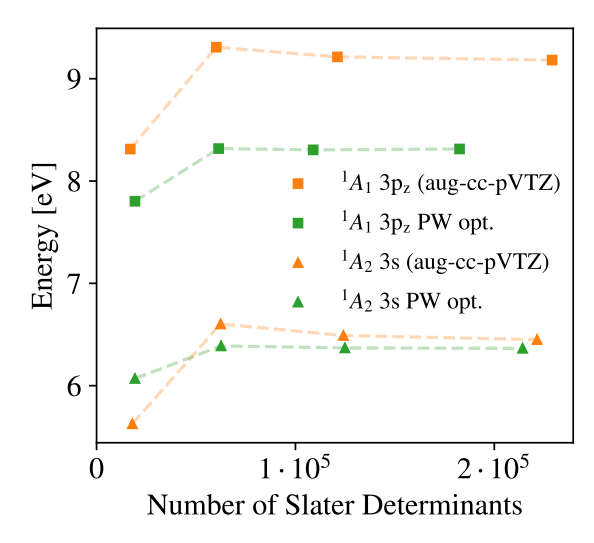


Figure 4: Convergence of the excitation energy for the 3s and  $3p_z$  Rydberg states of NH<sub>3</sub> with respect to the number of Slater determinants included in the NNCI calculation, in all cases generated from 52 MOs formed initially from the aug-cc-pVTZ basis set. The occupied orbitals are optimized in plane wave based Hartree-Fock calculations either for the ground state (orange) or the target excited state (green).

with  $10^5$  determinants, which is five orders of magnitude less than what a full CI calculation would require. Different from the 3s Rydberg state, the energy of the  $3p_z$  state is overestimated when the orbitals are optimized for the ground state. Further information on the convergence with respect to both the number of orbitals and determinants included in the NNCI can be found in the Supporting Information (SI).

#### 

The results of NNCI calculations for the  $H_2O$  molecule are shown in Fig. 5. The excitation energy obtained for the 3s,  $3p_x$  and  $3p_y$  states is shown and compared to experimental estimates  $^{28}$  as well as several high-level calculations. The x-axis is normal to the plane of the molecule. The agreement with the experimental measurements and with other theoretical values is good except for the GMS SU CCSD calculation  $^5$  of the  $3p_x$  state when the latter

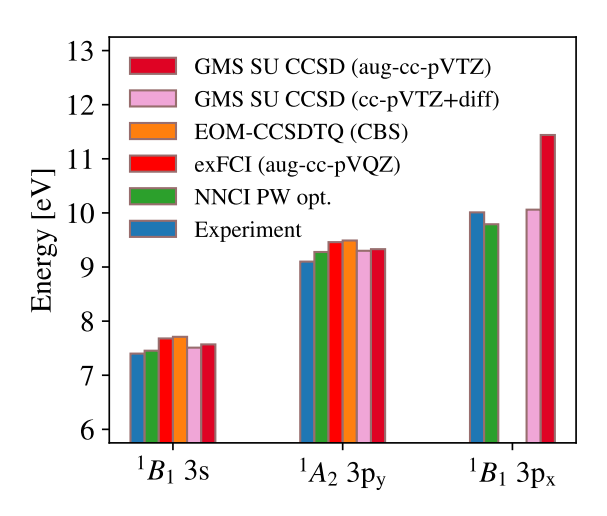


Figure 5: Comparison of NNCI calculated excitation energy for the 3s,  $3p_y$  and  $3p_x$  Rydberg states of H<sub>2</sub>O, based on 52 MOs initially formed from the aug-cc-pVTZ basis set but then optimized variationally for the target Rydberg state (NNCI PW opt), with experimentally measured <sup>28</sup> values, illustrating good agreement. Results of several other theoretical calculations are also shown: extrapolated full CI calculations (exFCI) based on the aug-ccpVQZ basis set, 4 EOM-CCSDTQ calculations in the complete basis set (CBS) limit, <sup>3</sup> available only for two of the states, as well as results of multireference GMS SU CCSD calculations<sup>5</sup> based on either a cc-pVTZ+diff basis set that includes extra diffuse functions, or the standard aug-cc-pVTZ basis set. The latter overly confines the  $3p_x$  leading to a large overestimate of the excitation energy, by more than 1 eV.

is based on the aug-cc-pVTZ basis. This is a high-level multireference (9R) calculation, but it is limited by the atomic basis set and the calculated excitation energy is significantly larger than the value obtained with NNCI where the occupied orbitals are optimized for the  $3p_x$  state. The difference is more than  $1\,\mathrm{eV}$ . This is analogous to the results for the  $3p_z$  state of the NH<sub>3</sub> molecule shown in Fig. 3 and can be ascribed to confinement of the Rydberg state by the atomic basis set. However, a GMS SU CCSD calculation with extra diffuse basis functions, cc-pVTZ+diff, gives a value of excitation energy close the results of the NNCI calculation. Again, this shows the advantage of vari-

ationally optimizing the orbitals for the target excited state in the plane wave based Hartree-Fock calculations. Even with the aug-cc-pVTZ basis for the initialization of the MOs, the results obtained with the NNCI calculations agree well with both experiment and high-level calculations with an extended atomic basis. EOM-CCSDTQ calculations in the complete basis set (CBS) limit from Ref. 3 are also in good agreement with the NNCI calculations of the 3s and  $3p_y$  Rydberg states, but analogous calculations for the  $3p_x$  Rydberg state are not available.

The limitation of the aug-cc-pVTZ basis for the 3p Rydberg states of  $H_2O$  has previously been demonstrated in the context of variational density functional calculations where a comparison was made with calculations using a real space grid. <sup>6</sup>

Fig. 6 illustrates the convergence of the NNCI calculation with respect to the number of NN cycles and the number of determinants included. In four cycles, convergence is reached already with 10<sup>5</sup> determinants, similar to the NH<sub>3</sub> calculation. Further details on the convergence are provided in the SI.

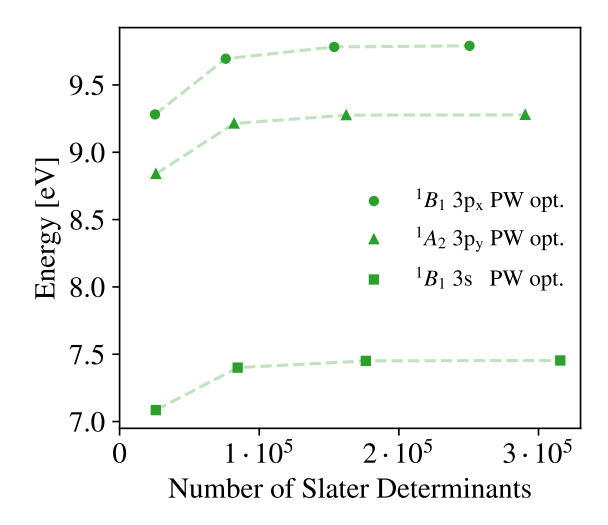


Figure 6: Convergence of the excitation energy for the 3s,  $3p_y$  and  $3p_x$  Rydberg states of  $H_2O$  with respect to the number of slater determinants included in the NNCI calculations, in all cases generated from 52 MOs formed initially from the aug-cc-pVTZ basis set. The occupied orbitals are optimized in plane wave calculations for the target excited state.

#### 4 Conclusion

The results presented here show two important aspects of CI calculations of excited states. First of all, faster convergence is obtained when the orbitals are variationally optimized for the target excited state in the Hartree-Fock calculations, here with a plane wave representation to overcome the limitations of typical atomic basis sets, such as aug-cc-pVTZ, when describing diffuse Rydberg states. Secondly, full CI results for the excitation energy can be obtained with several orders of magnitude fewer Slater determinants by using the NN-based selective CI. The NNCI method is extended here to calculations of excited electronic states and is shown to give accurate results for challenging Rydberg states of NH<sub>3</sub> and H<sub>2</sub>O molecules. Convergence is reached in four training/refinement NN iteration, leading to inclusion of 10<sup>5</sup> Slater determinants.

The optimization of the orbitals for the target excited state demonstrated here to be important in calculations of Rydberg states, can also be of advantage for other types of excited states, for example long-range charge transfer excitations. There, the orbitals can differ significantly between the ground states and an optimized excited state and the number of determinants needed to reach convergence in a selective CI calculation is expected to be significantly reduced by using optimized orbitals.

Acknowledgement This work was supported by the Icelandic Research Fund (grants nos. 2511544 and 2410644) and the University of Iceland Research Fund. GL acknowledges support from the ERC under the European Union's Horizon Europe research and innovation programme (grant no. 101166044, project NEXUS). Views and opinions expressed are however those of the author(s) only and do not necessarily reflect those of the European Union or ERC Executive Agency. Neither the European Union nor the granting authority can be held responsible for them. PB gratefully acknowledges the ARTEMIS funding via the QuantERA program of the European Union provided by German Federal Ministry of Education and Research under the grant 13N16360 within the program "From basic research to market". Y.L.A.S. acknowledges support by the Max Planck Society. Computer resources, data storage, and user support were provided by the Icelandic Research e-Infrastructure (IREI) funded by the Icelandic Infrastructure Fund. The authors further gratefully acknowledge the scientific support and HPC resources provided by the Erlangen National High Performance Computing Center (NHR@FAU) of the Friedrich-Alexander-Universität Erlangen-Nürnberg (FAU).

#### **Supporting Information**

The convergence of the energy of the ground and excited states as well as the excitation energy as a function of the number of Slater determinants and the number of molecular orbitals included in the NNCI calculations is illustrated in the Supporting Information.

#### References

- (1) Seidu, I.; Krykunov, M.; Ziegler, T. Applications of time-dependent and time-independent density functional theory to Rydberg transitions. *Journal of Physical Chemistry A* **2015**, *119*, 5107–5116.
- (2) Cheng, C. L.; Wu, Q.; Van Voorhis, T. Rydberg energies using excited state density functional theory. *Journal of Chemical Physics* **2008**, *129*, 124112.
- (3) Chrayteh, A.; Blondel, A.; Loos, P.-F.; Jacquemin, D. Mountaineering Strategy to Excited States: Highly Accurate Oscillator Strengths and Dipole Moments of Small Molecules. *J. Chem. Theory Comput.* **2021**, *17*, 416–438.
- (4) Loos, P.-F.; Scemama, A.; Blondel, A.; Garniron, Y.; Caffarel, M.; Jacquemin, D. A Mountaineering Strategy to Excited States: Highly Accurate Reference Energies and Benchmarks. J. Chem. Theory Comput. 2018, 14, 4360–4379.

- (5) Li, X.; Paldus, J. General-model-space state-universal coupled-cluster method: excitation energies of water. *Mol. Phys.* **2006**, *104*, 661–676.
- (6) Sigurdarson, A. E.; Schmerwitz, Y. L. A.; Tveiten, D. K. V.; Levi, G.; Jónsson, H. Orbital-optimized density functional calculations of molecular Rydberg excited states with real space grid representation and self-interaction correction. J. Chem. Phys. 2023, 159, 214109.
- (7) Schmerwitz, Y. L. A.; Levi, G.; Jónsson, H. Calculations of Excited Electronic States by Converging on Saddle Points Using Generalized Mode Following. J. Chem. Theory Comput. **2023**, 19, 3634.
- (8) Ivanov, A. V.; Levi, G.; Jónsson, E. Ö.; Jónsson, H. Method for Calculating Excited Electronic States Using Density Functionals and Direct Orbital Optimization with Real Space Grid or Plane-Wave Basis Set. J. Chem. Theory Comput. **2021**, 17, 5034–5049.
- (9) Levi, G.; Ivanov, A. V.; Jónsson, H. Variational Density Functional Calculations of Excited States via Direct Optimization. *J. Chem. Theory Comput.* **2020**, *16*, 6968–6982.
- (10) Schmerwitz, Y. L. A.; Thirion, L.; Levi, G.; Jónsson, E. Ö.; Bilous, P.; Jónsson, H.; Hansmann, P. A Neural-Network-Based Selective Configuration Interaction Approach to Molecular Electronic Structure. J. Chem. Theory Comput. 2025, 2301, 21.
- (11) Kossoski, F.; Loos, P.-F. State-Specific Configuration Interaction for Excited States. *Journal of Chemical Theory and* Computation **2023**, 19, 2258–2269.
- (12) Decleva, P.; Fronzoni, G.; Lisini, A.; Stener, M. Molecular orbital description of core excitation spectra in transition metal compounds. An ab initio CI calcultaion on

- TiCl4 and isoelectronic molecules. Chemical Physics 1994, 186, 1–16.
- (13) Blöchl, P. E. Projector augmented-wave method. *Phys. Rev. B* **1994**, *50*, 17953–17979.
- (14) Blöchl, P. E.; Först, C. J.; Schimpl, J. Projector augmented wave method:ab initio molecular dynamics with full wave functions. *Bull. Mater. Sci.* **2003**, *26*, 33–41.
- (15) Dunning, T. H. Gaussian basis sets for use in correlated molecular calculations. I. The atoms boron through neon and hydrogen. J. Chem. Phys. 1989, 90, 1007–1023.
- (16) Kendall, R. A.; Dunning, T. H.; Harrison, R. J. Electron affinities of the first-row atoms revisited. Systematic basis sets and wave functions. *J. Chem. Phys.* **1992**, *96*, 6796–6806.
- (17) Rossi, T. P.; Lehtola, S.; Sakko, A.; Puska, M. J.; Nieminen, R. M. Nanoplasmonics simulations at the basis set limit through completeness-optimized, local numerical basis sets. J. Chem. Phys. 2015, 142, 094114.
- (18) Larsen, A. H.; Vanin, M.; Mortensen, J. J.; Thygesen, K. S.; Jacobsen, K. W. Localized atomic basis set in the projector augmented wave method. *Phys. Rev. B* 2009, 80, 195112.
- (19) Ivanov, A. V.; Jónsson, E. Ö.; Vegge, T.; Jónsson, H. Direct energy minimization based on exponential transformation in density functional calculations of finite and extended systems. *Comput. Phys. Commun.* **2021**, *267*, 108047.
- (20) Mortensen, J. J.; Larsen, H.; M.; Ivanov, V.; Kuisma, Taghizadeh, A.; Peterson, A.; Haldar, A.; Dohn, A. O.; Schäfer, C.; Jónsson, E. O.; D.; Nilsson, Hermes, Ε. F. Kastlunger, G.; Levi, G.; Jónsson, H.; Häkkinen, H.; Fojt, J.; Kangsabanik, J.; Sødeguist, J.; Lehtomäki, J.; Heske, J.;

- Enkovaara, J.; Winther, K. T.; Dulak, M.; Melander, M. M.; Ovesen, M.; Louhivuori, M.; Walter, M.; Gjerding, M.; Lopez-Acevedo, O.; Erhart, P.; Warmbier, R.; Würdemann, R.; Kaappa, S.; Latini, S.; Boland, T. M.; Bligaard, T.; Skovhus, T.; Susi, T.; Maxson, T.; Rossi, T.; Chen, X.; Schmerwitz, Y. L. A.; Schiøtz, J.; Olsen, T.; Jacobsen, K. W.; Thygesen, K. S. GPAW: An open Python package for electronic structure calculations. J. Chem. Phys. 2024, 160, 092503.
- (21) Haynes, W. M.; Bruno, T. J.; Lide, D. R. CRC Handbook of Chemistry and Physics; Taylor & Francis Group, 2016.
- (22) Thirion, L.; Hansmann, P.; Bilous, P. SO-LAX: A Python solver for fermionic quantum systems with neural network support. *SciPost Phys. Codebases* **2025**, *51*, 1.
- (23) Bilous, P.; Thirion, L.; Menke, H.; Haverkort, M. W.; Pálffy, A.; Hansmann, P. Neural-network-supported basis optimizer for the configuration interaction problem in quantum many-body clusters: Feasibility study and numerical proof. *Phys. Rev. B* **2025**, *111*, 035124.
- (24) Kolos, W.; Wolniewicz, L. Theoretical Investigation of the Lowest Double-Minimum State E, F  $^{1}\Sigma_{g}^{+}$  of the Hydrogen Molecule. J. Chem. Phys. **1969**, 50, 3228–3240.
- (25) Wolniewicz, L.; Dressler, K. Adiabatic potential curves and nonadiabatic coupling functions for the first five excited  $^{1}\Sigma_{g}^{+}$  states of the hydrogen molecule. *J. Chem. Phys.* **1994**, 100, 444–451.
- (26) Skerbele, A.; Lassettre, E. N. Electronimpact spectra. J. Chem. Phys. 1965, 42, 395.
- (27) Arfa, M. B.; Tronc, M. Lowest energy triplet states of group Vb hydrides: NH<sub>3</sub> (ND<sub>3</sub>) and PH<sub>3</sub>. Chem. Phys. **1991**, 155, 143.

(28) Chutjian, A.; Hall, R. I.; Trajmar, S. Electron-impact excitation of  $H_2O$  and  $D_2O$  at various scattering angles and impact energies in the energy-loss range 4.2--12~eV. J. Chem. Phys. **1975**, 63, 892.

# Supporting Information for "Orbital Optimization and Neural-Network-Assisted Configuration Interaction Calculations of Rydberg States"

Gianluca Levi,\*, $^{\dagger,\ddagger}$  Max Kroesbergen, $^{\P}$  Louis Thirion, $^{\P,\dagger}$  Yorick L. A. Schmerwitz, $^{\dagger,\S}$  Elvar Ö. Jónsson, $^{\dagger}$  Pavlo Bilous, $^{\parallel}$  Philipp Hansmann, $^{*,\P,\dagger}$  and Hannes Jónsson\*, $^{\dagger}$ 

†Science Institute and Faculty of Physical Sciences, University of Iceland, Reykjavík,

Iceland

‡Department of Chemical and Pharmaceutical Sciences, University of Trieste, 34127

Trieste, Italy

¶Department of Physics, Friedrich-Alexander-Universität Erlangen/Nürnberg, 91058

Erlangen, Germany

§Max-Planck-Institut für Kohlenforschung, 45470 Mülheim an der Ruhr, Germany
||Max Planck Institute for the Science of Light, Staudtstraße 2, 91058 Erlangen, Germany

E-mail: gianluca.levi@units.it; philipp.hansmann@fau.de; hj@hi.is

The energy of the ground and excited state as well as the excitation energy as a function of the number of Slater determinants and the number of molecular orbitals included in the NNCI calculations is illustrated in the following figures.

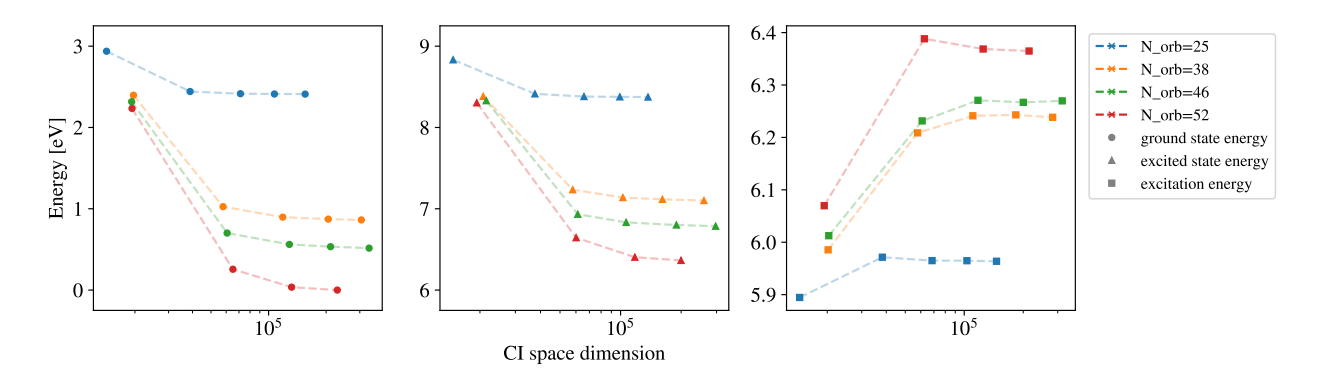


Figure S1: NNCI calculations related to the 3s Rydberg state of the NH<sub>3</sub> molecule using molecular orbitals optimized for the excited state. Left: ground-state energy. Middle: excited-state energy. Right: excitation energy.

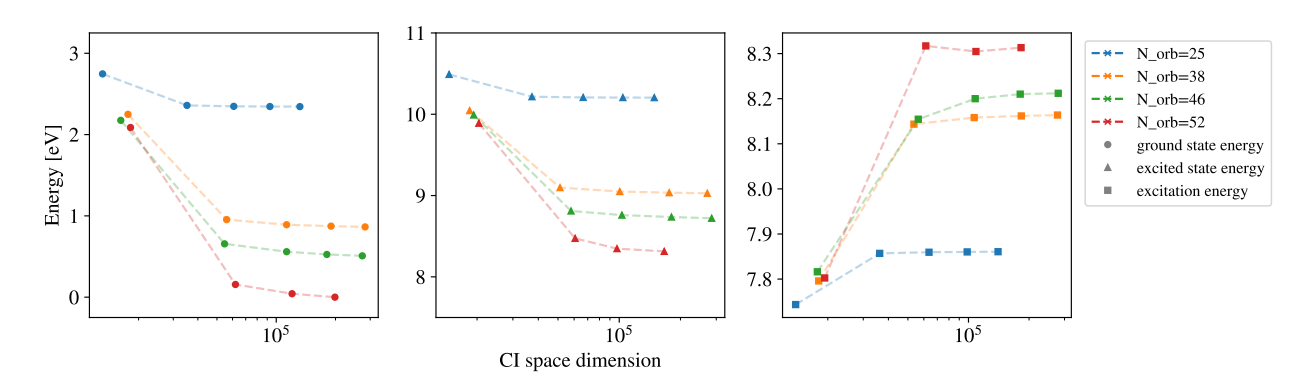


Figure S2: NNCI calculations related to the  $3p_z$  Rydberg state of the NH<sub>3</sub> molecule using molecular orbitals optimized for the excited state. Left: ground-state energy. Middle: excited-state energy. Right: excitation energy.

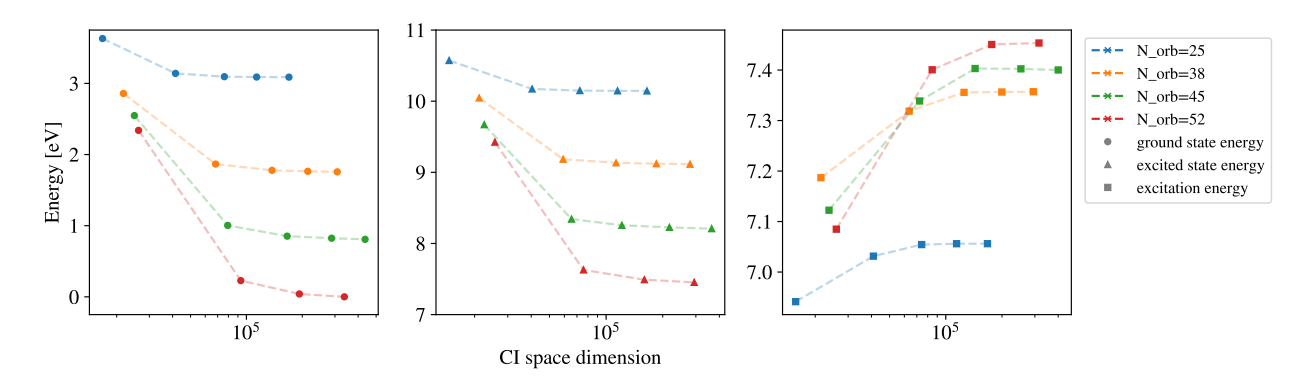


Figure S3: NNCI calculations related to the 3s Rydberg state of the  $H_2O$  molecule using molecular orbitals optimized for the excited state. Left: ground-state energy. Middle: excited-state energy. Right: excitation energy.

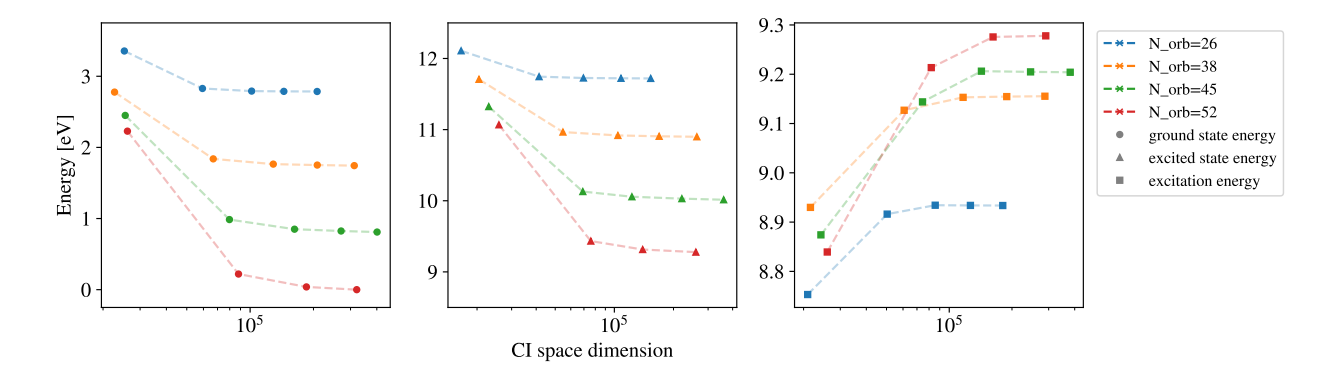


Figure S4: NNCI calculations related to the  $3p_y$  Rydberg state of the  $H_2O$  molecule using molecular orbitals optimized for the excited state. Left: ground-state energy. Middle: excited-state energy. Right: excitation energy.

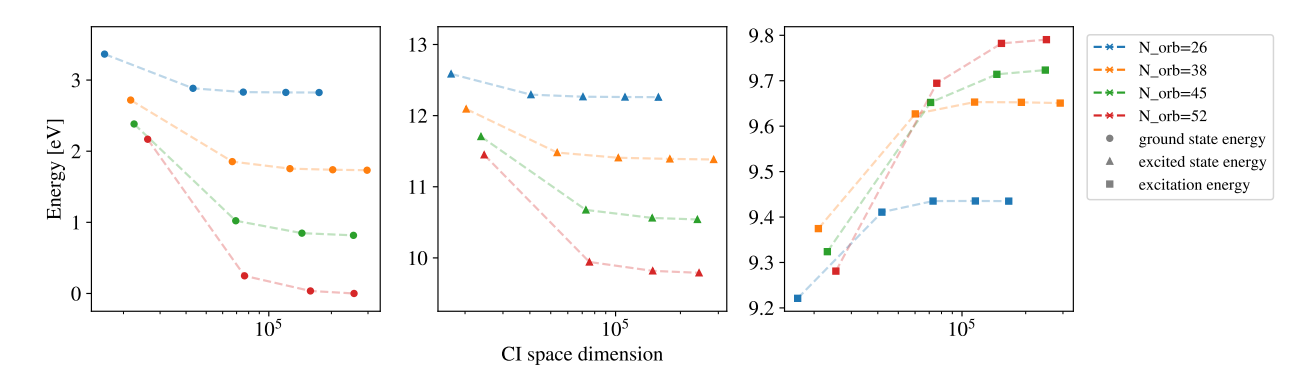


Figure S5: NNCI calculations related to the  $3p_x$  Rydberg state of the  $H_2O$  molecule using molecular orbitals optimized for the excited state. Left: ground-state energy. Middle: excited-state energy. Right: excitation energy.